



Time- vs. frequency-domain femtosecond surface sum frequency generation

Sylvie Roke^{*}, Aart W. Kleyn, Mischa Bonn

Leiden Institute of Chemistry, Leiden University, Einsteinweg 55, P.O. Box 9502, 2300 RA Leiden, Netherlands

Received 8 November 2002; in final form 6 January 2003

Abstract

We present an experimental and theoretical investigation into time- vs. frequency-domain femtosecond sum frequency spectroscopy at the metal–liquid interface. Although frequency and time-domain measurements are theoretically equivalent it is demonstrated here experimentally that the two approaches are sensitive to different physical aspects of the system and provide complementary information. Time-domain measurements are demonstrated to be more clearly influenced by the inhomogeneity of adsorption sites, since the decay of the vibrational polarization can be mapped directly. A generalization of existing models allows for the simultaneous description of both frequency and time-domain measurements.

© 2003 Elsevier Science B.V. All rights reserved.

Vibrational sum frequency generation (SFG) is a powerful surface specific probe of molecules at interfaces. It has been used to study gas–metal [1–3] (applying fs to ns laser pulses) and also liquid–metal interfaces [4–7] (applying ps and ns pulses) that are of importance for e.g., catalysis or electrochemistry. The strength of the technique is that it directly interrogates the vibrational modes of the adsorbed molecule, leading to detailed insights in the binding, structure, and vibrational dynamics of the metal–adsorbate system. The recent extension of this technique to the fs regime enables not only frequency multiplexing experiments [8–10], but also time-domain measurements

[11,12]. In addition, since the pulse duration (typically ~ 100 fs) is appreciably shorter than the decay of the vibrational polarization (dephasing time or inverse linewidth), this decay can be mapped directly in the time-domain.

Hence, information about the polarization decay can be obtained either by performing a time-domain measurement or indirectly from the linewidth in a frequency-domain spectrum. After an ultrashort fs-infrared pulse creates a macroscopic polarization, its decay can be probed in two ways, as illustrated in Fig. 1. In a frequency-domain measurement the infrared polarization is upconverted using a spectrally narrow (temporally long) visible pulse. The (homogeneous) spectral linewidth (2Γ) is directly related to the vibrational dephasing time T_2 ($\Gamma = 1/T_2$). In a time-domain experiment the polarization is upconverted using a

^{*} Corresponding author. Fax: +31-71-5274451.

E-mail address: roke@chem.leidenuniv.nl (S. Roke).

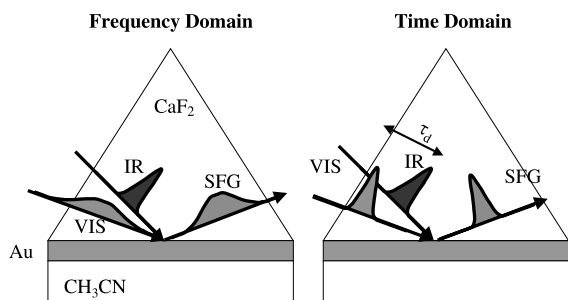


Fig. 1. Schematic illustration of a frequency-domain (left) and a time-domain (right) SFG experiment. In a frequency-domain experiment, temporally long (spectrally narrow) VIS pulses are used to upconvert the IR-induced polarization at the surface and the time integrated signal is recorded as a function of frequency. In the time-domain experiment, short pulses are employed, and the frequency-integrated SFG signal is recorded as a function of delay time between IR and VIS pulses.

temporally short (spectrally broad) pulse and the integrated SFG intensity is measured as a function of delay time (τ_d) between the infrared and visible pulse. In this way the time evolution of the vibrational polarization, commonly referred to as free induction decay (FID), is observed in real-time. Since in both schemes the polarization decay is detected, the polarization measured in the time-domain is the Fourier transform of the frequency-domain result.

We demonstrate that, although both measurement schemes are therefore theoretically equivalent, the time-domain experiments are inherently more sensitive to the lineshape as the non-resonant metal response can be separated from the resonant molecular response. We illustrate this with time-domain and frequency-domain measurements of homogeneously and inhomogeneously distributed oscillators (the C–H and C–N stretch vibration of liquid acetonitrile (CH_3CN) on an amorphous gold surface). We adapt existing models to elucidate the vibrational decay mechanism and describe both time-domain and frequency-domain measurements within one formalism.

The SFG experiments are performed using 120 fs FWHM Gaussian pulse duration infrared pulses ($10 \mu\text{J}$ energy FWHM spectral bandwidth of 220 cm^{-1}) centered at 2940 and 2250 cm^{-1} for investigating the C–H and C–N stretch mode of acetonitrile, respectively. The temporal and spectral

profile of the 800 nm visible pulse ($2.3 \mu\text{J}$, repetition rate reduced from 1 kHz to 83 Hz) was varied using a pulse-shaper: frequency-domain SFG spectra are recorded with a 3 cm^{-1} FWHM bandwidth ($>10 \text{ ps}$ auto-correlate) upconversion pulse and time-domain FID's are measured with 120 fs visible pulses. Switching from time-domain to frequency-domain measurements only requires the insertion of a slit in the pulse-shaper, leaving the alignment unchanged. For a meaningful comparison, we have used identical energies of the visible pulse in the frequency-domain and time-domain experiments. Note that it is straightforward to increase the signal in the time-domain measurement, by increasing the pulse energy (only $2.3 \mu\text{J}$ is used in the experiment). In the frequency-domain measurement, increasing the pulse energy cannot be done without sacrificing spectral resolution, for our type of experimental set-up. The measurements were done in a co-propagating total internal reflection geometry (after [5,13]) in which the reflected SFG field is detected (see Fig. 1). The p-polarized IR (VIS) pulses are incident under 57° (61°) with respect to the surface normal. The 3 nm thick Au films are prepared by vapor deposition on the face of a 60° CaF_2 prism. This produces thin (high resistivity) films with a roughness determined by the substrate [14]. The absorbed fluence was kept well below the ablation threshold ($\sim 1.7 \text{ mJ/cm}^2$, as determined both experimentally and from a two temperature model calculation, see e.g., [15]) and prior to each measurement the signal of the non-resonant $\text{CaF}_2/\text{Au}/\text{air}$ interface was checked to make sure that the layer was not damaged. The signal of a purposely damaged gold layer is dramatically lower. Thus it was ensured that the experiments presented here were performed on intact, homogeneous gold layers.

The top panel of Fig. 2 shows an SFG spectrum in the C–H stretch region of an acetonitrile/gold interface and an air/gold interface. The main peak from the acetonitrile/gold interface corresponds to the symmetric C–H stretch vibration of the CH_3 stretch vibration of acetonitrile [14]. The measured SFG spectra can be reproduced very well with the calculated SFG intensity ($I_{\text{SFG}}(\omega)$) expressed in terms of the second-order non-linear polarization ($P^{(2)}$), which is the product of the second-order

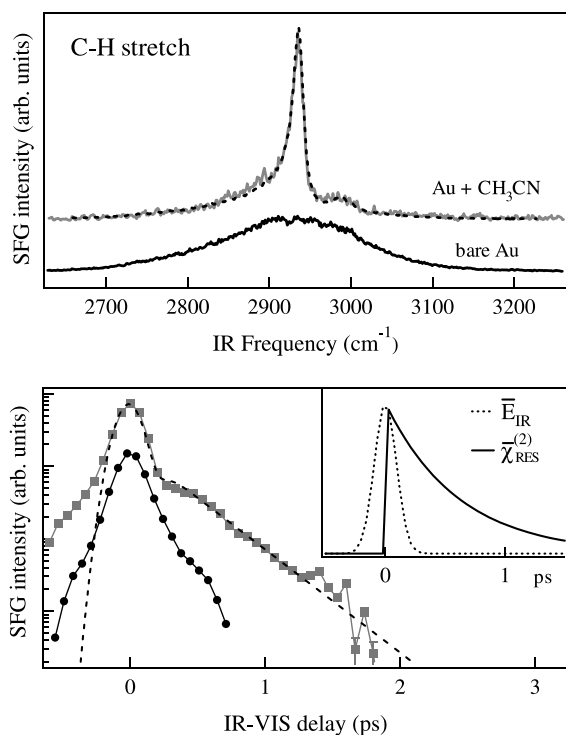


Fig. 2. Frequency-domain and time-domain SFG measurements in the C–H stretch region of acetonitrile. Top panel: SFG spectra of a clean Au film (lower spectrum) and a Au film with acetonitrile. The weak feature around 3000 cm^{-1} corresponds to the asymmetric stretch vibration. Lower panel: free induction decay of a clean Au film (offset) and a Au film with acetonitrile. The dashed lines in both panels are fits to the data with very similar T_2 's (see text). The inset shows $\bar{E}_{\text{IR}}(t)$ and $\bar{\chi}_{\text{RES}}^{(2)}(t)$.

non-linear susceptibility ($\chi^{(2)}$), the infrared $E(\omega_{\text{IR}})$ and visible $E(\omega_{\text{VIS}})$ fields [1,2]:

$$I_{\text{SFG}}(\omega) \propto |P^{(2)}(\omega)|^2 \propto |\chi^{(2)}(\omega)|^2 = |\chi_{\text{RES}}^{(2)}(\omega) + \chi_{\text{NR}}^{(2)}(\omega)|^2 \quad (1)$$

$$\chi_{\text{RES}}^{(2)} = \frac{A}{((\omega - \omega_0) - i\Gamma)}; \quad \chi_{\text{NR}}^{(2)} = A_0 e^{i\phi}$$

with ω_0 the resonance frequency, 2Γ the spectral FWHM linewidth and ϕ the phase difference between the resonant and non-resonant SFG fields. The response of the interface consists of a resonant term ($\chi_{\text{RES}}^{(2)}$) to describe the interaction of the light with the vibrational mode and a non-resonant term ($\chi_{\text{NR}}^{(2)}$), due to the instantaneous response of the metal to the light. $\chi_{\text{RES}}^{(2)}$ is usually modeled as a

Lorentzian response. The non-resonant contribution can be extracted from the gold/air SFG spectrum. The dashed line in Fig. 2 is a fit to the data using this model, resulting in $\omega_0 = 2939\text{ cm}^{-1}$ and $\Gamma = 8.0\text{ cm}^{-1}$ corresponding to $T_2 = 0.66\text{ ps}$.

The lower panel of Fig. 2 shows a time-domain measurement of the same vibration. This FID consists of both a non-resonant (instantaneous) and a resonant (decaying) contribution. The same measurement is also shown for a clean gold surface, which is the cross-correlate of the incoming pulses and allows for determining the time resolution of the experiment. It can immediately be seen that the decay of the resonant signal is exponential, with a slope of $3.2\text{ THz} (= 2/T_2)$, corresponding to $T_2 = 0.61\text{ ps}$, in good agreement with the frequency-domain analysis. To reproduce the FID, we follow the procedure first described by Owrutski et al. [2]. The SFG intensity (I_{SFG}) as a function of delay time (τ_d) between the infrared and visible fields can be calculated from the time-dependent polarization $P^{(2)}(t, \tau_d)$, as

$$I_{\text{SFG}}(\tau_d) = \int_{-\infty}^{\infty} |P^{(2)}(t, \tau_d)|^2 dt, \quad (2)$$

$$P^{(2)}(t, \tau_d) = \bar{E}_{\text{VIS}}(t - \tau_d) \left\{ \alpha \int_{-\infty}^t \bar{E}_{\text{IR}}(t') \bar{\chi}_{\text{RES}}^{(2)}(t - t') dt' + \beta \bar{E}_{\text{IR}}(t) e^{i\phi} \right\} e^{i(\omega_{\text{IR}} + \omega_{\text{VIS}})t} + \text{c.c.} \quad (3)$$

The first term between brackets in Eq. (3) describes the resonant interaction of the infrared field with the adsorbate (with a magnitude α), where $\bar{\chi}_{\text{RES}}^{(2)}(t)$ is the time dependent envelope of the response of the adsorbate. The second term describes the non-resonant instantaneous response of the gold surface to the infrared field with a magnitude β and a phase difference ϕ with respect to the resonant polarization. $\bar{E}_{\text{IR}}(t)$ and $\bar{E}_{\text{VIS}}(t)$ are the IR and VIS fields envelopes. The frequency-domain Lorentzian response implies single exponential decay in the time-domain. Indeed using Eq. (2), with $\bar{\chi}_{\text{RES}}^{(2)}(t) = e^{-t/T_2}$ and $T_2 = 0.61\text{ ps}$ results in excellent agreement between data and model (see the fit in the lower panel of Fig. 2). It should be noted that the bandwidth of the upconversion pulse is negligible compared to the vibrational linewidths.

Very contrasting behaviour is observed for the C–N stretch vibration of acetonitrile on gold [14]. Fig. 3 shows both the SFG spectrum (top panel) and the FID (lower panel). This spectrum can be reproduced very well with Eq. (1), setting $\omega_0 = 2250 \text{ cm}^{-1}$ and $\Gamma = 7.6 \text{ cm}^{-1}$ ($T_2 = 0.68 \text{ ps}$). As both the SFG spectrum and the FID are a measurement of the same polarization, the FID should be described with the time-domain equivalent (Fourier transform) of the frequency-domain response. However an exponentially decaying $\bar{\chi}_{\text{RES}}^{(2)}(t)$ and $T_2 = 0.68 \text{ ps}$ (the calculated FID, shown as dashed line in the lower panel of Fig. 3) clearly does not describe the measured FID.

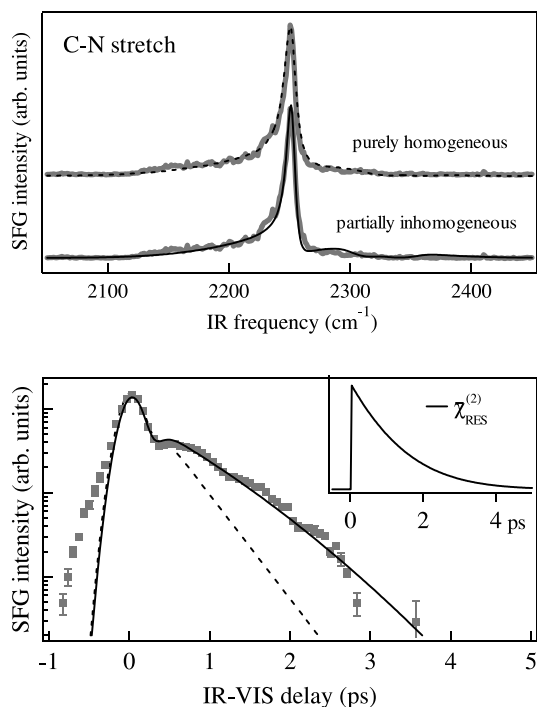


Fig. 3. Frequency-domain and time-domain SFG measurements in the C–N stretch region of acetonitrile. Top panel: two (identical) SFG spectra of a Au film with acetonitrile. The upper (lower) spectrum is fitted assuming a homogeneous (inhomogeneous) distribution of adsorption sites. Lower panel: free induction decay of a Au film with acetonitrile. The data shown consists of an average of nine different data sets, of which the error bars show the spread. The dashed (solid) line is a calculation assuming a homogeneous (inhomogeneous) distribution of adsorption sites (see text). The inset shows $\bar{\chi}_{\text{RES}}^{(2)}(t)$ used in Eq. (3).

Apparently, obtaining a good fit with the commonly employed Eq. (1) is not a guarantee for homogeneous dephasing behaviour. The clear non-exponential decay of the FID seems to suggest a partially inhomogeneous scenario, in which the resonance frequency is not the same for all molecules but varies with the adsorption site¹.

Following [7,16,17], such a partially inhomogeneous distribution of adsorption sites can be characterized by a Gaussian distribution, $g(\omega'_0)$, of resonance frequencies (ω'_0) centered around ω_{inh} with a width $\Delta\omega$, i.e., $g(\omega'_0) = 2/(\Delta\omega\sqrt{\pi}) e^{-((\omega'_0 - \omega_{\text{inh}})^2/(\Delta\omega)^2)}$. The time-domain resonant response can then be written as

$$\begin{aligned} \chi_{\text{RES}}^{(2)}(t) &= \sum_{\omega'_0} \chi_{\text{RES}}^{(2)}(t, \omega'_0) \\ &= \int_0^\infty d\omega'_0 g(\omega'_0) e^{-t/T_2} e^{i(\omega'_0 + \omega_{\text{VIS}})t} + \text{c.c.} \\ &\equiv \bar{\chi}_{\text{RES}}^{(2)}(t) \cos(\omega_{\text{inh}} + \omega_{\text{VIS}})t \end{aligned} \quad (4)$$

which consists of a time dependent envelope $\bar{\chi}_{\text{RES}}^{(2)}(t)$ and an oscillating frequency $\omega_{\text{inh}} + \omega_{\text{VIS}}$. For the frequency range of interest, the envelope can be approximated by $\bar{\chi}_{\text{RES}}^{(2)}(t) = e^{-t/T_2} e^{-t^2(\Delta\omega/2)^2}$, as long as $\Delta\omega/\omega_{\text{inh}} \ll 1$. This is a generalized version of the commonly used equation to fit SFG spectra. The amount of inhomogeneity is determined by the product $\Delta\omega T_2$; $\Delta\omega T_2 \ll 1$ describes a homogeneous scenario (obtained by setting $g(\omega'_0) = \delta(\omega'_0 - \omega_0)$), whereas $\Delta\omega T_2 \gg 1$ yields a totally inhomogeneous distribution of sites. To obtain the frequency-domain polarization, we take the Fourier transform of $P^{(2)}(t, \tau_d = 0)$ and regard the visible field as a CW field.

Applying Eqs. (2)–(4) to calculate the FID and the upper part of Eq. (1) in combination with the Fourier transform of Eq. (4) to reproduce the spectrum yields the fits in Fig. 3. Using the same dephasing time ($T_2 = 1.65 \text{ ps}$) and frequency distribution ($\omega_{\text{inh}} = 2250 \text{ cm}^{-1}$ and $\Delta\omega = 2.8 \text{ cm}^{-1}$, $\Delta\omega T_2 = 0.6$), both the SFG spectrum and the FID can be reproduced very well with one set of

¹ An exponential fit to the TD measurement results in a FD FWHM linewidth of 6.6 cm^{-1} , which is significantly too narrow.

parameters. That this is a unique set of parameters can be seen from the functional form of $\overline{\chi}_{\text{RES}}^{(2)}(t)$ immediately. Namely, the function in the exponent is a unique function. This directly translates to the uniqueness of $\overline{\chi}_{\text{RES}}^{(2)}(t)$ itself. To illustrate this, Fig. 4 shows three calculated SFG spectra and FID's for two different sets of $\Delta\omega$ and T_2 . $\Delta\omega = 2.8 \text{ cm}^{-1}$ and $T_2 = 1.65 \text{ ps}$ corresponds to the best fit. The degree of inhomogeneity, $\Delta\omega$, was varied by a factor of 2, and T_2 was treated as a fitting parameter. It clearly demonstrates that the time-domain allows for a more accurate estimate of T_2 and $\Delta\omega$ than the frequency-domain. The error in the derived values for $\Delta\omega$ and T_2 are determined by the signal-to-noise ratio in the tail of the FID, and amount to $\Delta\omega = 2.8 \pm 1 \text{ cm}^{-1}$ and $T_2 = 1.65 \pm 0.4$

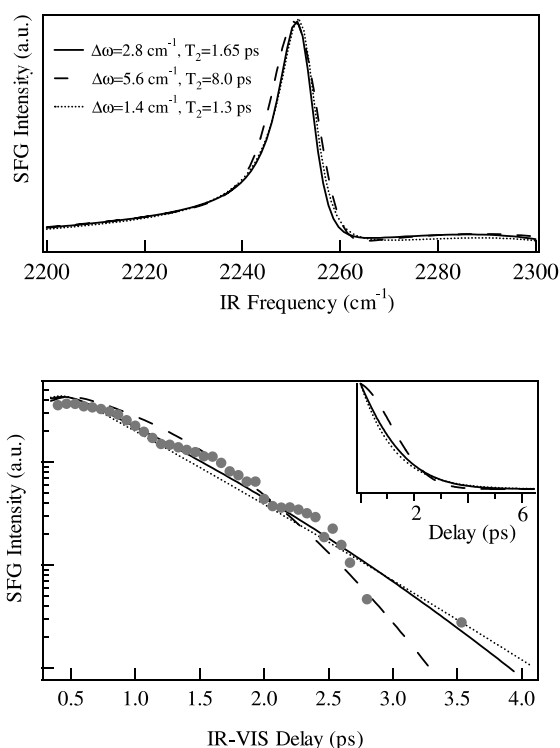


Fig. 4. Calculated frequency-domain (top panel) and time-domain SFG spectra (bottom panel) in the C–N stretch region of acetonitrile for different values of $\Delta\omega$ and T_2 . The solid line corresponds to the fit in Fig. 3. $\Delta\omega = 1.4 \text{ cm}^{-1}$, $T_2 = 1.3 \text{ ps}$ corresponds to a more homogeneous scenario (\cdots) and $\Delta\omega = 5.6 \text{ cm}^{-1}$, $T_2 = 8.0 \text{ ps}$ corresponds to a more inhomogeneous scenario ($-\cdot-$). The time-domain data is also shown. The inset shows $\overline{\chi}_{\text{RES}}^{(2)}(t)$ changing shape.

ps. For totally inhomogeneous dephasing behaviour however, the frequency-domain spectrum can be decisive, as it should be totally symmetric around ω_{inh} .

From the above analysis the following conclusions can be drawn:

(1) Although the SFG spectrum and the FID both map the macroscopic polarization at the surface, the time-domain measurement is much more sensitive to the spectral lineshape. It is inherently more sensitive to the molecular response than the frequency-domain measurement, since the non-resonant signal is only present when the two short pulses overlap. Thus, for IR–VIS delay $>0.5 \text{ ps}$ the time-domain FID is governed solely by the decay of the resonant polarization. In contrast, the frequency-domain SFG spectrum does not give an unobscured image of the resonant polarization, since the molecular polarization *always* interferes with the non-resonant metal response. Therefore, independent of the lineshape model employed, a theoretical description of the frequency-domain data will always have one extra parameter, namely the phase difference between the resonant and non-resonant response. Apart from an extra fitting parameter, the frequency-domain SFG spectra can also be distorted due to the large dispersion in the refractive index of acetonitrile around the resonance [5]. This effect will be present in the interference region and hence can cause appreciable distortion to the frequency-domain spectrum. Moreover, from an experimental point of view, the signal-to-noise in the time-domain experiment can be increased more easily than the signal-to-noise in the frequency-domain experiment.

(2) Even with a partially inhomogeneous distribution of adsorption sites it is still possible to determine the homogeneous dephasing time. The above model only assumes an exponentially decaying set of resonances with a Gaussian frequency distribution. Such an approach, however, includes an assumption regarding the distribution and is not a direct measurement of inhomogeneous effects, like a photon echo experiment.

(3) Considering only the frequency-domain data, it is clear that obtaining a good fit assuming a Lorentzian response is not a guarantee for homogeneous dephasing behaviour.

In summary, although frequency-domain and time-domain SFG experiments are theoretically equivalent, they can lead to different conclusions concerning the lineshape. To elucidate the vibrational decay mechanism both time and frequency-domain measurements should be conducted and analyzed in a detailed fashion.

Acknowledgements

The authors would like to thank R.C.V. van Schie and P. Schakel for excellent technical support. This work is part of the research program of the Foundation for Fundamental Research on Matter (FOM), which is financially supported by the Netherlands Organization for Scientific Research (NWO), and was supported in part by a fellowship for M.B. from the Royal Netherlands Academy of Arts and Sciences (KNAW).

References

- [1] J.H. Hunt, P. Guyot-Sionnet, Y.R. Shen, *Chem. Phys. Lett.* 133 (1987) 189.
- [2] J.C. Owrutski, J.P. Culver, M. Li, Y.R. Kim, M.J. Sarisky, M.S. Yeganeh, A.G. Yodh, R.M. Hochstrasser, *J. Chem. Phys.* 97 (1992) 4421.
- [3] A.L. Harris, A. Rothberg, L.H. Dubois, N.J. Levinos, L. Dhar, *Phys. Rev. Lett.* 64 (1990) 2086.
- [4] G.R. Bell, Z.X. Li, C.D. Bain, P. Fisher, D.C. Duffy, *J. Phys. Chem. B* 101 (1998) 9461.
- [5] C.T. Williams, Y. Yang, C.D. Bain, *Langmuir* 16 (2000) 2343.
- [6] S. Baldeli, G. Mailhot, P. Ross, Y.R. Shen, G.A. Somorjai, *J. Phys. Chem. B* 105 (2001) 654.
- [7] C.D. Bain, P.B. Davies, T.H. Ong, R.N. Ward, M.A. Brown, *Langmuir* 7 (1991) 1563.
- [8] E.W.M. van der Ham, Q.H.F. Vreken, E.R. Eliel, *Surf. Sci.* 386 (1996) 96.
- [9] L.J. Richter, T.P. Petrali-Mallow, J.C. Stephenson, *Opt. Lett.* 23 (1998) 1594.
- [10] D. Star, T. Kikteva, G.W. Leach, *J. Chem. Phys.* 111 (1999) 14.
- [11] M. Bonn, C. Hess, S. Funk, J.H. Miners, B.N.J. Persson, M. Wolf, G. Ertl, *Phys. Rev. Lett.* 84 (2000) 4653.
- [12] S. Roke, A.W. Kleyn, M. Bonn, *J. Phys. Chem. A* 105 (2001) 1683.
- [13] S.R. Hatch, R.S. Polizzotti, S. Dougal, P. Rabinowitz, *Chem. Phys. Lett.* 196 (1992) 97.
- [14] S. Roke, A.W. Kleyn, M. Bonn, submitted (2003).
- [15] M. Bonn, D.N. Denzler, S. Funk, M. Wolf, S.-S. Wellerhof, J. Hohlfeld, *Phys. Rev. B* 61 (2000) 1101.
- [16] P. Guyot-Sionnest, *Phys. Rev. Lett.* 66 (1991) 1489.
- [17] M. van der Voort, C.W. Rella, L.F.G. van der Meer, A.V. Akimov, J.I. Dijkhuis, *Phys. Rev. Lett.* 84 (2000) 1236.